NeuroImage 200 (2019) 450–459

Contents lists available at ScienceDirect

NeuroImage

journal homepage: www.elsevier.com/locate/neuroimage

Modulation of the spontaneous hemodynamic response function across levels of consciousness

Guo-Rong Wu [a,b], Carol Di Perri [c,d], Vanessa Charland-Verville [c], Charlotte Martial [c], Manon Carrière [c], Audrey Vanhaudenhuyse [c], Steven Laureys [c,1], Daniele Marinazzo [b,*,1]

[a] Key Laboratory of Cognition and Personality, Faculty of Psychology, Southwest University, Chongqing, 400715, China
[b] Department of Data Analysis, University of Ghent, B9000, Ghent, Belgium
[c] Coma Science Group, GIGA Research Center, University of Liège, B4000, Liège, Belgium
[d] Center for Clinical Brain Sciences, Centre for Dementia Prevention, UK Dementia Research Institute, University of Edinburgh, EH16 4SB, Edinburgh, United Kingdom

A B S T R A C T

Functional imaging research has already contributed with several results to the study of neural correlates of consciousness. Apart from task-related activation derived in fMRI, PET based glucose metabolism rate or cerebral blood flow account for a considerable proportion of the study of brain activity under different levels of consciousness. Resting state functional connectivity MRI is playing a crucial role to explore the consciousness related functional integration, successfully complementing PET, another widely used neuroimaging technique. Here, spontaneous hemodynamic response is introduced to characterize resting state brain activity giving information on the local metabolism (neurovascular coupling), and useful to improve the time-resolved activity and connectivity measures based on BOLD fMRI. This voxel-wise measure is then used to investigate the loss of consciousness under Propofol anesthesia and unresponsive wakefulness syndrome. Changes in the hemodynamic response in precuneus and posterior cingulate are found to be a common principle underlying loss of consciousness in both conditions. The thalamus appears to be less obviously modulated by Propofol, compared with frontoparietal regions. However, a significant increase in spontaneous thalamic hemodynamic response was found in patients in unresponsive wakefulness syndrome compared with healthy controls. Our results ultimately show that anesthesia- or pathology-induced neurovascular coupling could be tracked by modulated spontaneous hemodynamic response derived from resting state fMRI.

1. Introduction

In order to provide effective assistance to diagnosis, prognosis, and assess potential treatments, it is crucial to understand the physiological basis of consciousness in pathological or pharmacological coma. Advanced neuroimaging techniques have significantly expanded our knowledge of neural correlates of consciousness level in human brain. For instance, FDG-PET imaging and fMRI have shown that altered activity, metabolism, and connectivity in thalamus, frontoparietal and default mode networks (Laureys, 2005; Laureys et al., 2000a, 2000b, 2002, 2004) are found in patients with disorders of consciousness; these findings have complemented the information on modulation of brain rhythms specific to alterations in consciousness from electrophysiological techniques (Gugino et al., 2001; Vijayan et al., 2013). A clinical validation study suggested that PET imaging could have a higher diagnostic precision than event-related fMRI in disorders of consciousness (Stender et al., 2014). This calls for an improved mining of the dynamic information by means of advanced fMRI models, considering the superior spatiotemporal resolution of fMRI.

Consciousness has two major components: awareness of environment and of self (i.e. the content of consciousness), and wakefulness (i.e. the level of consciousness) (Laureys, 2005). The vegetative state, redefined as unresponsive wakefulness syndrome (UWS) is the most dramatic model of dissociation between wakefulness and awareness. Patients in unresponsive wakefulness syndrome are awake but seemingly not aware. In the last decade neuroimaging studies on these patients have extensively investigated the neural correlates of awareness, mainly exploring the correlation between awareness and global brain function (Laureys et al., 1999b), regional brain function, brain activation induced by passive external stimulation (Laureys and Schiff, 2012) or mental imagery task (Owen et al., 2005), and changes in resting state connectivity (Laureys et al., 1999a, 1999b, 2000b). Similar approaches have also been applied to identify the neural correlates of different states of consciousness as induced by anesthetic drugs manipulation (Boveroux et al., 2010; DiFrancesco et al., 2013; Hudetz, 2012). Compared to global brain metabolism, regional metabolic dysfunction is a more reliable maker of individual conscious-unconscious state transition (Laureys, 2005). Studies of passive stimuli have shown promising results, especially for

* Corresponding author. Ghent University, Department of Data Analysis, 2 Henri Dunantlaan, B9000, Ghent, Belgium.
E-mail address: daniele.marinazzo@ugent.be (D. Marinazzo).
[1] joint last authors.

https://doi.org/10.1016/j.neuroimage.2019.07.011
Received 6 March 2019; Received in revised form 3 July 2019; Accepted 4 July 2019
Available online 5 July 2019

minimally conscious state patients, but the neuronal responses cannot be always stable (Laureys and Schiff, 2012); as a consequence inference of cognitive function from these cerebral activations is controversial (Menon et al., 1999; Schiff and Plum, 1999). Resting state functional connectivity (FC) plays a critical role in the quantification of brain function integration sustaining the state of consciousness (Boveroux et al., 2010; Laureys et al., 1999a, 1999b, 2000b). Although it well confirmed previous FDG-PET findings (Laureys and Schiff, 2012), it is increasingly known that BOLD-based approaches are susceptible to some limitations, such as the neurovascular connection anatomy (Tak et al., 2014) and motion artifacts (Power et al., 2012), which may contribute to high proportion of the resting state FC signal commonly detected by BOLD fMRI.

BOLD-fMRI hemodynamic response describes the vascular oxygenation changes following a neuronal impulse response, complementing PET, being less invasive and with a better spatial and temporal resolution, but less relatable to local metabolism. Here we propose another possible marker of cerebral activity under altered levels of consciousness, which can be connected to vascular and metabolic processes: we investigate the shape pattern of the hemodynamic response using resting state fMRI data in UWS patients and healthy subjects under Propofol sedation. The hemodynamic response correlates of consciousness will be explored and compared between UWS and anesthesia. Apart from being a local biomarker, the hemodynamic response affects activation and connectivity (Gitelman et al., 2003; Rangaprakash et al., 2018). A subject- and voxel-vise estimation of its shape would allow a better estimate of these latter measures. Previous PET (Boly et al., 2011; Laureys, 2005; Laureys et al., 2004) and fMRI studies (Guldenmund et al., 2013) reported that thalamus, fronto-parietal cortical areas, salience network and default mode network (DMN) exhibit state-dependent spontaneous hemodynamic response in the resting state. We will here aim to verify if these local modulations are replicated with the proposed measure.

2. Materials and methods

2.1. Subjects

Two datasets, referred to as the Propofol and the UWS one in the paper, were used in this study. Twenty-one healthy right-handed volunteers were included in the Propofol dataset. Twenty UWS patients and thirty-two healthy controls (HC) participated in the UWS study. Diagnosis of UWS was made after repeated behavioral assessments by experienced and trained neuropsychologists using the Coma Recovery Scale-Revised (CRS-R (Giacino et al., 2004; Wannez et al., 2017);). Written informed consent to participate in the study was obtained from the healthy subjects and from the legal representatives of the patients. None of the healthy subjects had a history of head trauma or surgery, mental illness, drug addiction, asthma, motion sickness, or previous problems during anesthesia. The study was approved by the Ethics Committee of the Medical School of the University of Liège (University Hospital, Liège, Belgium). The relevant demographic and clinical information can be found in Table 1 and Table 2. For the UWS dataset, no statistically significant differences in age and sex were found between the control group and the patients' one.

2.2. Functional data acquisition

The Propofol dataset considered in the current study has first been analyzed in (Boveroux et al., 2010). Functional MRI acquisition consisted of resting-state fMRI volumes repeated in four clinical states only for 21 healthy volunteers: normal wakefulness (W1), mild sedation (S1), deep sedation (S2), and recovery of consciousness (W2). The temporal order of mild- and deep-sedation conditions was randomized. The typical scan duration was half an hour in each condition. The number of scans per session was matched in each subject to obtain a similar number of scans in all four clinical states (mean ± SD, 251 ± 77 scans/session).

Table 1
Demographics test for all subjects. a: Chi-Square goodness of fit test; b: Pearson's Chi-square test for independence.

	UWS (n = 13)	Healthy Controls (n = 25)	Propofol (n = 21)
Age (y)	Mean = 42.8 SD = 16.5 $t(36) = 0.0011$, $p = 0.9991$	Mean = 42.8 SD = 15.7	Mean = 23.4 SD = 4.2
Sex	M = 7 F = 6 $\chi^2(1) = 0.08$ $p = 0.78$[a] $\chi^2(1) = 0.37$, $p = 0.54$[b]	M = 16 F = 9 $\chi^2(1) = 1.96$ $p = 0.16$[a]	M = 5 F = 16 $\chi^2(1) = 5.76$ $p = 0.02$

Table 2
Demographics and accident etiology for UWS patients.

Patient	Sex	Age (y)	Accident Etiology
sub01	F	44	anoxia
sub02	M	15	TBI
sub03	M	54	post meningitis a pneumococcus
sub04	F	38	anoxia
sub05	M	33	intracranial hemorrhage
sub06	M	28	mixed TBI-anoxia
sub07	M	43	anoxia
sub08	F	69	anoxia
sub09	F	57	TBI
sub10	M	73	TBI
sub11	F	31	TBI
sub12	F	36	anoxia
sub13	M	36	anoxia

There is only one session of resting state fMRI for each subject in the UWS dataset, each one containing 300 scans.

All functional images were acquired on a 3 T S Allegra scanner (Siemens AG, Munich, Germany);

Propofol dataset: Echo Planar Imaging sequence using 32 slices; repetition time (TR) = 2460 ms, echo time = 40 ms, field of view = 220 mm, voxel size = 3.45 × 3.45 × 3 mm, and matrix size = 64 × 64 × 32).

UWS dataset: Echo Planar Imaging sequence using 32 slices; repetition time (TR) = 2000 ms, echo time = 30 ms, field of view = 220 mm, voxel size = 3.44 × 3.44 × 3 mm, and matrix size = 64 × 64 × 32).

2.3. Data preprocessing

All structural images in both datasets were manually reoriented to the anterior commissure and segmented into grey matter, white matter (WM), cerebrospinal fluid (CSF), skull, and soft tissue outside the brain, using the standard segmentation option in SPM 12. Then a study-based template was created, in order to minimize deformity due to atrophic brains.

Resting-state fMRI data preprocessing was subsequently carried out using both AFNI and SPM12 packages. First, slice time correction was performed on EPI volumes. Then the images were realigned to the first volume for head-motion correction. 8 UWS patients and 7 healthy control subjects were excluded from the dataset because either translation or rotation exceeded ±1.5 mm or ±1.5°, or mean framewise displacement (FD) exceeded 0.5, resulting in 13 UWS patient and 25 healthy controls which were used in the analysis, and 22 sessions in Propofol group subjects were also excluded. The resulting volumes were then despiked using AFNI's 3dDespike algorithm to mitigate the impact of outliers. The mean BOLD image across all realigned volumes was coregistered with the structural image, and the resulting warps applied to all the despiked BOLD volumes. Finally, all the coregistered BOLD images were smoothed (8 mm full-width half-maximum) and spatially normalized into MNI 152

space.

Several parameters were simultaneously included in a linear regression to remove possible spurious variances from the data. These were i) six head motion parameters obtained in the realigning step, ii) non-neuronal sources of noise estimated using the anatomical component correction method (aCompCor, the representative signals of no interest from subject-specific WM and CSF included the top five principal components from WM and the top five from CSF mask) (Behzadi et al., 2007), iii) first-order Legendre polynomial. Then the residual time series were temporally band-pass filtered (0.008–0.1 Hz).

2.4. Spontaneous point process event and HRF retrieval

We employed a blind hemodynamic response function (HRF) retrieval technique specially developed for resting-state BOLD-fMRI signal (Wu et al., 2013), which considers the latter as driven by spontaneous point process events. A linear time-invariant model for the observed resting state BOLD response is assumed (Boynton et al., 1996; Dale and Buckner, 1997). We consider a common HRF is shared across the various spontaneous point process events at a given voxel, to ensure a more robust estimation. The BOLD-fMRI signal $y(t)$ at a particular voxel is given by:

$$y(t) = h(t) \otimes x(t) + \varepsilon(t) \quad \varepsilon \tilde{} N(0, \sigma^2 V) \tag{1}$$

where $x(t)$ is the sum of time-shifted delta functions, centered at the onset of each spontaneous point process event and $h(t)$ is the (unknown) hemodynamic response to these events, $\varepsilon(t)$ represents additive noise and $\otimes$ denotes convolution. The noise errors are not independent in time due to aliased biorhythms and unmodelled neural activity, and are accounted for using an AR(p) model during the parameter estimation (we set $p = 2$ in current study). In practice, $y(t)$ is not sampled continuously in time, but rather at discrete intervals, i.e. multiples of repetition time (TR). Following this mapping, the convolution was performed in TR temporal resolution in a previous study (Wu et al., 2013). On the other hand, given that spontaneous point process event onsets do not need to be synchronized with scans, here we adapted the original algorithm and performed the convolution at a higher temporal resolution, with N time points per scan, then down-sampled to TR temporal resolution in Equation (2). The lag between the peak of neural activation and the peak in BOLD response is assumed to be $k \times \frac{TR}{N}$ seconds (where $0 < k < PST \times \frac{N}{TR}$, $N = 11$ in the current study; PST indicates the peristimulus time). The timing set S of these resting-state BOLD transients is defined as the time points exceeding a given threshold around a local peak, and can be defined as: $S\{i\} = t_i,\ y(t_i) \geq m \,\&\, y(t_i) \geq y(t_i \pm \tau)$, where we set $\tau = 1, 2$ and $m = \mu + \sigma$ (μ and σ are the mean and standard deviation of the time series). The optimal time lags can be obtained by minimizing the mean squared error of equation (1), i.e. the optimization problem:

$$\widehat{h}, \widehat{k} = \underset{h,k}{\operatorname{argmin}} y(t) - h(t)\widehat{x}(t) \tag{2}$$

$$\widehat{x}(t-k) = \begin{cases} 1, & t \in S \\ 0, & t \notin S \end{cases} \quad 0 < k \leq \mathrm{PST}$$

In order to avoid pseudo-point process events induced by motion artifacts, a temporal mask with FD < 0.3 was added to exclude these high movement frames from the timing set S by means of scrubbing (Power et al., 2012).

In its general form, the method described above makes no assumptions about the exact shape or functional form of the hemodynamic responses. However, application of prior knowledge about possible hemodynamic response shapes could reduce the bias in the linear estimation framework especially for the low signal noise ratio dataset, and sharply reduce the computational cost. Here we assume that the hemodynamic response for all resting state spontaneous point process events and at all locations in the brain are fully contained in a d-dimensional linear sub-space H of $\Re^d$, then, any hemodynamic response h can be represented uniquely as the linear combination of the corresponding basis vectors. The canonical HRF in SPM with its delay and dispersion derivatives (i.e. informed basis set) are employed as the basis functions in current study (Friston et al., 1998).

To characterize the shape of hemodynamic response, three parameters of the HRF, namely response height, time to peak, Full Width at Half Maximum (FWHM), were estimated, which could be interpretable in terms of potential measures for response magnitude, latency and duration of neuronal activity (Lindquist and Wager, 2007). In Fig. 1 some results are summarized, evidencing the BOLD point processes with the pseudo-events generating them.

To quantify the influence of model fitting on HRF analysis, the Pearson correlation between the preprocessed BOLD signal and the fitted BOLD signal was evaluated. Then we performed statistical analyses on the Fisher-transformed correlation maps, namely within-subject ANOVA for propofol dataset and independent t-test for UWS dataset. No significant difference was found (the group mean correlation maps are shown in Fig. S1).

The toolbox to perform these analyses (in Matlab, Python, Docker Container, and BIDS app) is freely available on the NITRC page https://www.nitrc.org/projects/rshrf.

2.5. Statistical analysis

We retrieved resting state HRF for all the voxels contained within the cerebrum using the AAL template (Tzourio-Mazoyer et al., 2002). HRF parameters for each subject were entered into a random-effects analysis (one-way ANOVA) within subjects, with three covariates (age, sex and mean FD) to identify regions which showed significant activity differences among four clinical states, a linear t contrast was computed, searching for a linear relationship between HRF and the level of consciousness across the four conditions (contrast (W1, W2, S1, S2): $y = -x - \frac{1}{4}\sum_{i=0}^{3}(-i)$ [1.5 0.5–1.5 -0.5]) (Boveroux et al., 2010). Nonlinear contrasts were also tested, with consistent results (see the supplementary material). A pairwise t-test between W1 and S2 (the two extreme states) was further performed to compare the results with those obtained from the UWS dataset.

A two-sample t-test with three covariates (age, sex and mean FD (Power et al., 2012)) was implemented to map group difference of HRF parameters between control subjects and UWS patients.

Additionally, independent statistical tests in the response height, time-to-peak, and FWHM can lead to potential false differences in the shape of the HRF. Statistical inference on the HRF was also performed with a multivariate analysis program 3dMVM in AFNI (Chen et al., 2015). However, missing data for a within-subject factor, or whether within-subject covariates vary across the levels of a within-subject factor cannot be handled with 3dMVM. We only applied 3dMVM on the UWS dataset, with HRF parameters (Response height, FWHM, Time to peak) as the within-subjects factor, and group as a between-subjects factor (healthy controls vs. UWS), age, sex and mean FD as the covariates.

The consistent group difference maps from the two different datasets were obtained using conjunctions (minimum statistic compared to the conjunction null) (Nichols et al., 2005).

Type I error due to multiple comparisons across voxels was controlled by family-wise error rate (Chumbley et al., 2010). Statistical significance for group analysis was set at $P_{FWE}<0.05$, derived from Gaussian random field theory.

The unthresholded statistical maps, as well as the median maps for all the parameters, are uploaded to NeuroVault.org https://neurovault.org/collections/4902/.

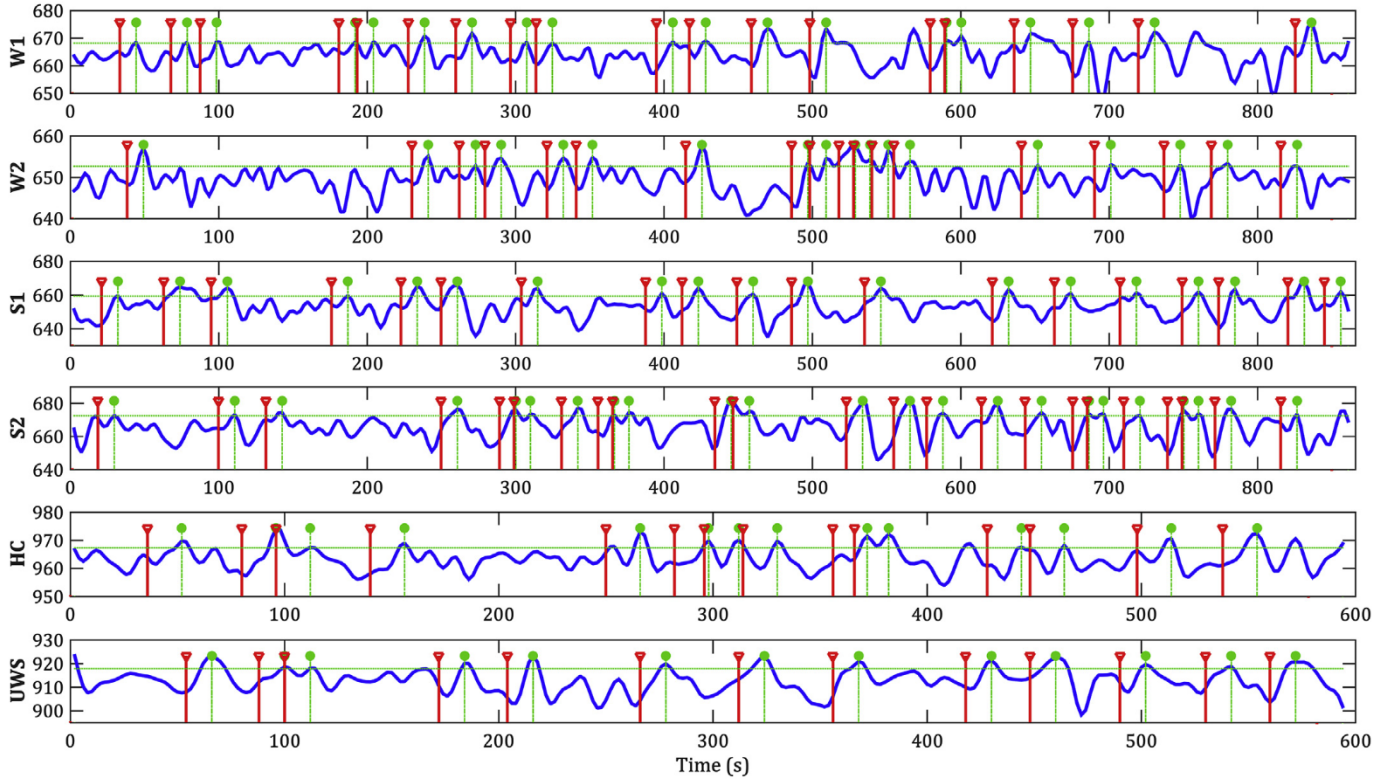

Fig. 1. Retrieval of point processes and pseudo-event times: the green horizontal dashed line represent the threshold ($\mu + \sigma$), the green stems represent the point process, the red stems indicate the pseudo neural events onset times (lagging behind the BOLD point processes). Each signal shown here comes from one voxel in the precuneus, the first four rows represent the same voxel for the same subject. Due to motion some above-threshold time points have been "scrubbed".

3. Results

3.1. Spatial distributions of resting state HRF parameters

The temporal interval between spontaneous point process events is inhomogeneously distributed (Fig. 2), a feature that enables a more robust GLM estimation for HRF retrieval. HRF parameters of each voxel are estimated and mapped on the brain (Fig. 3). The median maps of each HRF parameters exhibit spatial heterogeneity across different level of consciousness and HRF models (Fig. 3). Similar distributions are present in W1, W2, and control group, higher response height and FWHM appear in frontal lobe and precuneus.

3.2. Group HRF differences and conjunction

Statistical maps of HRF parameters reveal that HRF shape parameters are modulated by Propofol anesthesia (Figs. 4 and 5.AB). We only report here the result from a linear contrast (the same used in (Boveroux et al., 2010)), the results from a nonlinear contrast are largely similar (Figs. S2 and S3). The linear covariation between HRF shape and the level of consciousness is mostly evident in the response height, and in specific brain areas: frontal lobe (middle/medial/inferior/superior frontal gyrus), anterior cingulate, inferior/superior parietal lobule, precuneus, posterior cingulate, supramarginal gyrus, angular gyrus, precentral/postcentral gyrus (primary somatosensory/motor cortex), supplementary motor area, superior/middle temporal gyrus, insula, parahippocampus, hippocampus.

Group pairwise differences between the two most extreme cases (W1 and S2) show a similar spatial distribution (Fig. 4).

A linear relationship with consciousness level was also found in FWHM in the frontal gyrus (medial/middle/inferior/superior) and anterior cingulate (Fig. 5A). No association (linear or nonlinear) was found between the temporal latency of hemodynamic response and consciousness level.

The UWS subjects show lower spontaneous response height than control subjects in precuneus, posterior cingulate, cuneus, inferior parietal lobule, supramarginal gyrus, and angular gyrus, but higher response height in putamen, thalamus, parahippocampus gyrus, fusiform, and anterior cingulate, while the sub-regions of frontal gyrus exhibit opposite patterns in spontaneous hemodynamic response height between UWS and control group (Fig. 6). In contrast to the UWS group, the control subjects show broader response width (FWHM) in precuneus, posterior cingulate, inferior parietal lobule, supramarginal gyrus (Fig. 5C). No group difference is found in the time to peak of hemodynamic response. The multivariate model results evidence a similar main effect on HRF parameters (Fig. S4).

A conjunction analysis for (*W1 minus S2*) and (*Control minus UWS*) contrasts yields a significant cluster of higher spontaneous HRF response height in precuneus and posterior cingulate (Fig. 7).

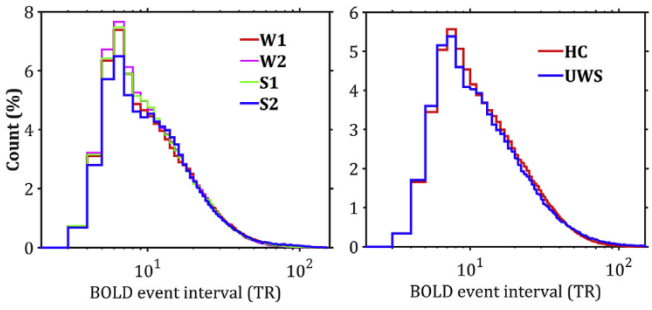

Fig. 2. Group level frequency distribution of temporal intervals between adjacent point process events. Left: Propofol dataset; Right: UWS dataset.

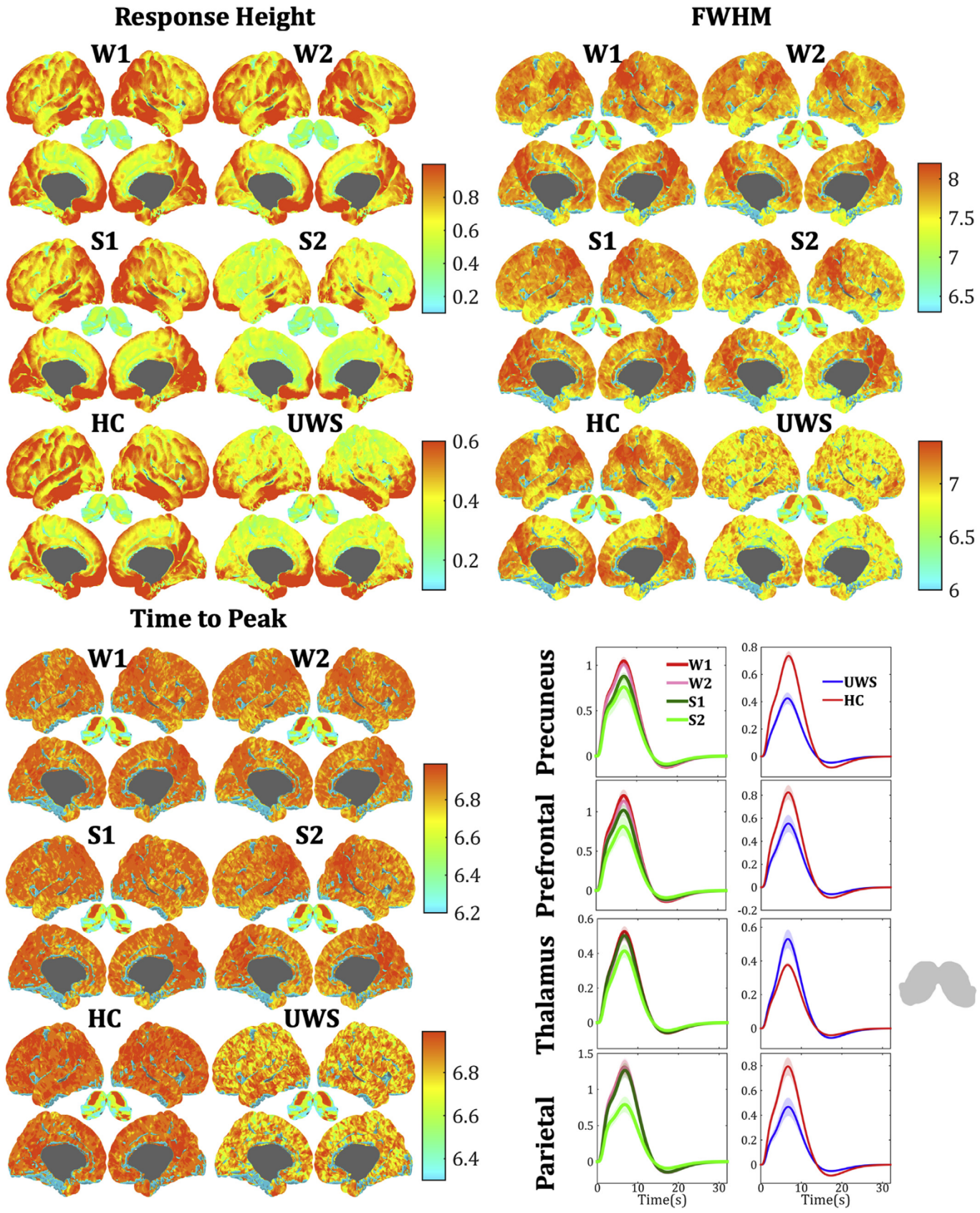

Fig. 3. Median maps of HRF parameters (response height, FWHM, time to peak), estimated by informed basis set. Different scales are used for each dataset and HRF parameter, while the same scale is used for the same HRF parameter and dataset. For better comparison, the maximum value in colormap is not the maximum value of HRF parameters. The thalamus is shown on a separate inset map. The lower right panel reports the group averaged HRF as percent signal change with its standard error in four representative locations (precuneus, MNI coordinates [-3, −60, 27]; thalamus, MNI coordinates [-9, −9, 3]; prefrontal, MNI coordinates [51,39,18]; parietal, MNI coordinates [-45, −57, 51]). The left column depicts results from the Propofol dataset, the right one from the UWS dataset.

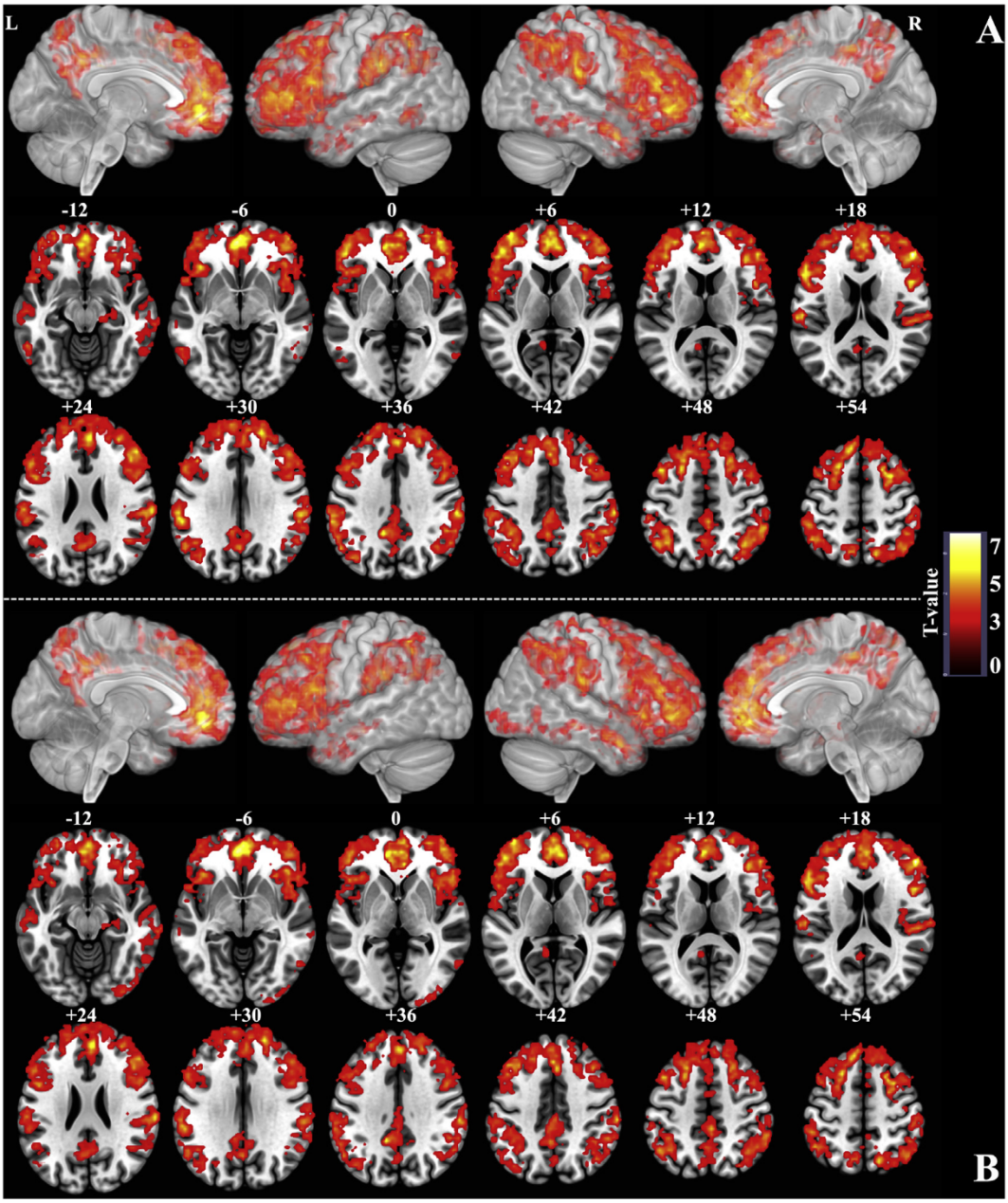

Fig. 4. (A) Linear correlation between response height and four levels of consciousness (W1, W2, S1, S2); (B) Response height differences between W1 and S2. $p < 0.05$, topo FWE correction.

4. Discussion

We investigated the modulations induced by changing levels of consciousness in resting state hemodynamic response based on BOLD fMRI signals in healthy control with Propofol anesthesia and UWS patients. This allowed us to explore the dissociation between wakefulness and awareness, present in UWS but not in anesthesia, from the point of view of a measure that is relevant both to the dynamics (local and integrated), and to the local metabolism.

The hemodynamic response showed both similarities and differences in pharmacological and pathologically induced loss of consciousness. We found that a modulation of hemodynamic response in precuneus and posterior cingulate is a common principle underlying loss of consciousness induced by Propofol anesthesia and UWS, which is consistent with previous PET and functional connectivity MRI studies (Fiset et al., 2005; Laureys, 2005). The hemodynamic response in frontoparietal networks is clearly altered with Propofol anesthesia, but changes in subcortical regions like the thalamus are not as evident. However, the spontaneous thalamic hemodynamic response exhibits distinctly different characteristic between healthy controls and UWS patients.

It is well established that most anesthetic agents decrease glucose metabolism in a dose-dependent manner with variable effect on glucose metabolism rate (GMR) and cerebral blood flow (CBF) (Alkire and Miller, 2005), while the BOLD-fMRI signal reflect the complex interactions between cerebral metabolic rate of oxygen, cerebral blood flow and volume (Ogawa et al., 1990). Therefore, the changes that occur in the brain metabolism and CBF caused by neural activity could be accompanied by concurrent changes in BOLD effect in a predictable way. Most fMRI studies employ active or passive paradigm to detect activation in sensory or cognitive system (Laureys and Schiff, 2012). However the quantifiable nature of relation between cerebral metabolism and resting state BOLD-HRF has been left largely unexplored.

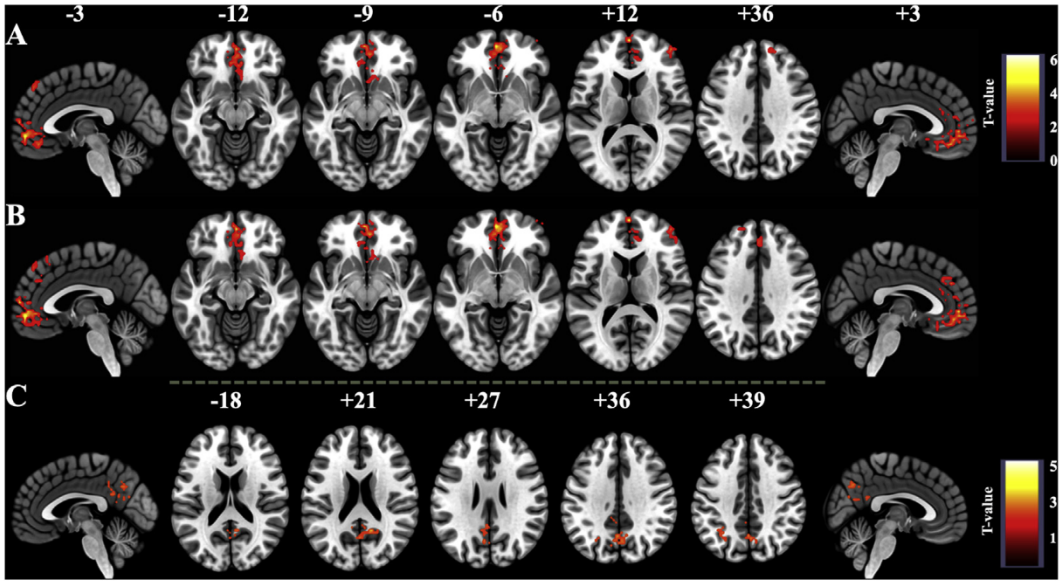

Fig. 5. (A) linear correlation between FWHM and four levels of consciousness (w1, w2, s1, s2), $p < 0.05$, topo FWE correction. (B) FWHM differences between W1 and S2. (C) Group differences of FWHM between healthy controls and UWS patients, $p < 0.05$, topo FWE correction.

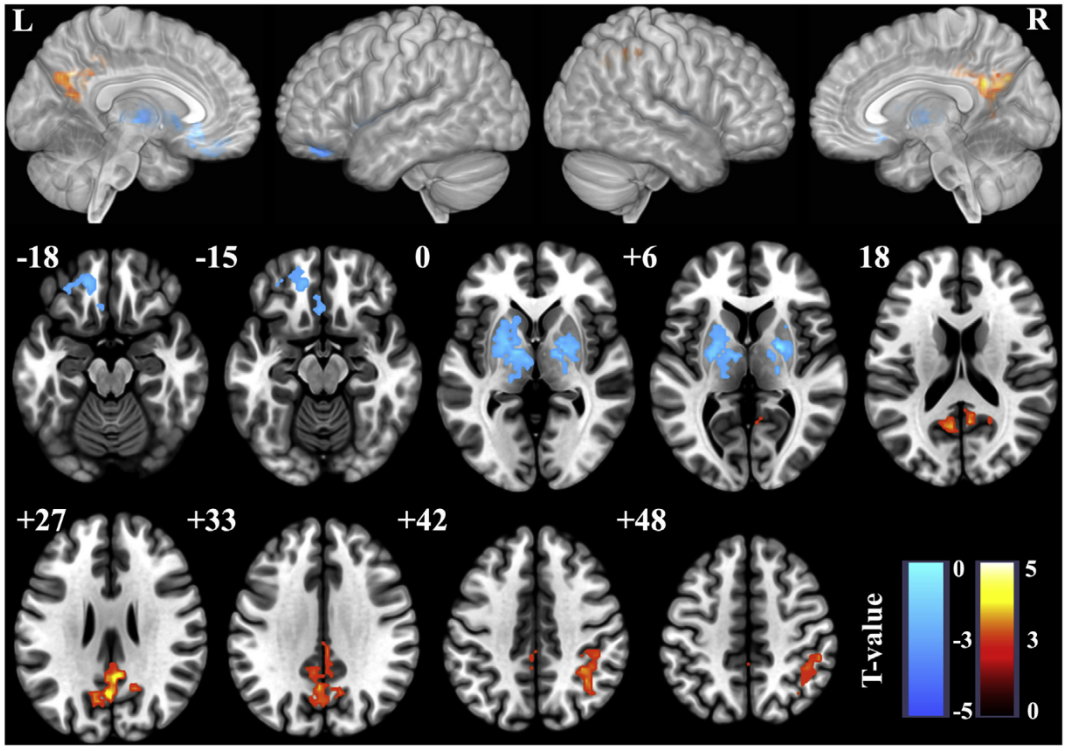

Fig. 6. Response height differences between healthy controls and UWS patients, $p < 0.05$, topo FWE correction.

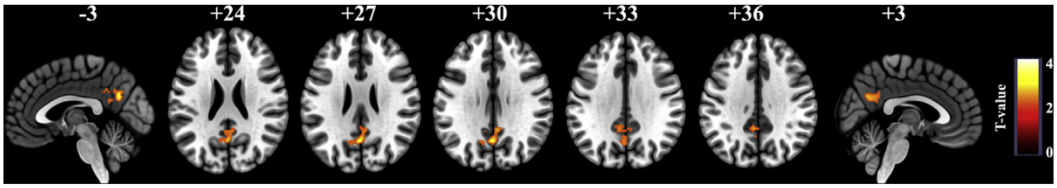

Fig. 7. Conjunction map of W1 minus S2 and healthy control minus UWS patients in response height differences, $p < 0.05$, topo FWE correction.

Several studies focused on regional GMR and CBF with PET to measure anesthesia or pathology induced unconsciousness (Alkire and Miller, 2005; Laureys, 2005). In the unconscious state, the regions that show consistent relative decreases of metabolism and blood flow are in the frontoparietal networks, DMN, as well as the thalamus (Alkire and Miller, 2005; Laureys et al., 2004; Nakayama et al., 2006). These regions are involved in conscious processing, thus a suggested mechanism connected to loss of consciousness could be a disturbance in the optimal balance between segregation and integration among these regions and those connected with them. DMN is considered to be involved in stimulus-independent thought, mind-wandering and self-consciousness (Raichle, 2015). The posterior cingulate cortex (PCC) and the medial precuneus are prominent features of the DMN, they act as core hubs in integrating information across functionally segregated brain regions, and display elevated metabolic activity in the resting state. PCC has dense structural connectivity to widespread brain regions, is involved in internally directed thought (Leech et al., 2012), and engaged in continuous information gathering and representation of the self and external world with interconnected precuneus and medial prefrontal cortices (Gusnard et al., 2001). The precuneus is one of the first regions of the brain to resume activity when regaining consciousness, and together with the adjacent PCC mostly differentiates patients in minimally conscious states from those in UWS (Laureys et al., 2004). Therefore, the consistent evidence of decreased hemodynamic response in precuneus and posterior cingulate speaks to deficits in cognitive functioning and information integration possibly leading to a breakdown of consciousness.

A BOLD-fMRI study on brain activation by auditory word stimulus during Propofol sedation suggested that the superior and middle temporal gyri and the inferior parietal lobule are involved in the formation of both implicit and explicit memories (Quan et al., 2013). The present results suggest that this kind of findings could be (partly) explained by modulations in the hemodynamic response.

The thalamus plays an important role in normal arousal regulation (Schiff, 2008), and is generally considered as the common locus of action of both brain dysfunction in UWS and general anesthetics. Its anatomy and physiology imply a central role in consciousness (Ward, 2011). However, thalamic depression in anesthesia may depend on the agent studied and the degree of sedation. It has been suggested that cortical cells are more sensitive to the effect of Propofol than sub-cortical elements (Alkire and Miller, 2005; Sun et al., 2008). Our findings support this evidence, revealing that spontaneous hemodynamic response in the frontal lobe is significantly correlated with the level of Propofol anesthesia, while the cluster size for the same effect in the thalamus was nonsignificant. Nonetheless, significant positive linear correlation with hemodynamic response height in thalamus could be found with small volume correction, as well as some negative linear correlation in part of the thalamus ($p < 0.05$, uncorrected, Fig. 8); higher hemodynamic response was only observed in UWS compared with healthy controls. These results though do not imply that the thalamic activity is not suppressed by Propofol. The Propofol effect might indeed mediate the thalamocortical interaction (Alkire et al., 2008), as suggested in a previous study on this dataset (Boveroux et al., 2010), showing that the thalamocortical connectivity in default network and bilateral executive-control networks were correlated with Propofol-induced decrease of consciousness. An increase in FC between the thalamus and the auditory cortex, insular cortex, primary somatosensory cortex, primary motor cortex, and supplementary motor area was observed with mild sedation (Guldenmund et al., 2013). In addition, the hyperactivity in thalamus is consistent with limbic hyperconnectivity in UWS shown in a previous study (Di Perri et al., 2013). This may reflect the correlation between alpha activity increases and spontaneous hemodynamic response (Brown et al., 2010; Wu and Marinazzo, 2015). The evident decrease of spontaneous hemodynamic responses in decreased states of consciousness offers a strong empirical support that thalamus is a hub for the neurobiology of consciousness.

It is worth to mention that the possible relationship between resting state FC and brain activity reflected by hemodynamic response in the pathological or pharmacological coma remains unclear. Hyperconnectivity or hypoconnectivity only indicate changes of synchronous cortical activity among brain areas, which may be induced by only one region or both of them; further analysis on hemodynamic response in each area could clearly explain the link between brain connectivity and activity (Tomasi and Volkow, 2018). The effects of hemodynamic variability on resting state FC have been investigated (Rangaprakash et al., 2018), as well as their implications for posttraumatic stress disorder (Rangaprakash et al., 2017) and autism (Yan et al., 2018). In addition, we must be careful when interpreting the present results. Indeed, it is worth noting that the loss of consciousness induced by pharmacological drugs involving a progressive loss of consciousness using controlled dosages or rather provoked by a pathologic disorder of consciousness resulting of severe brain insults of various origins may differ regarding the underlying dynamics. Nevertheless, this comparison provides a unique opportunity to explore the dissociation between wakefulness and awareness.

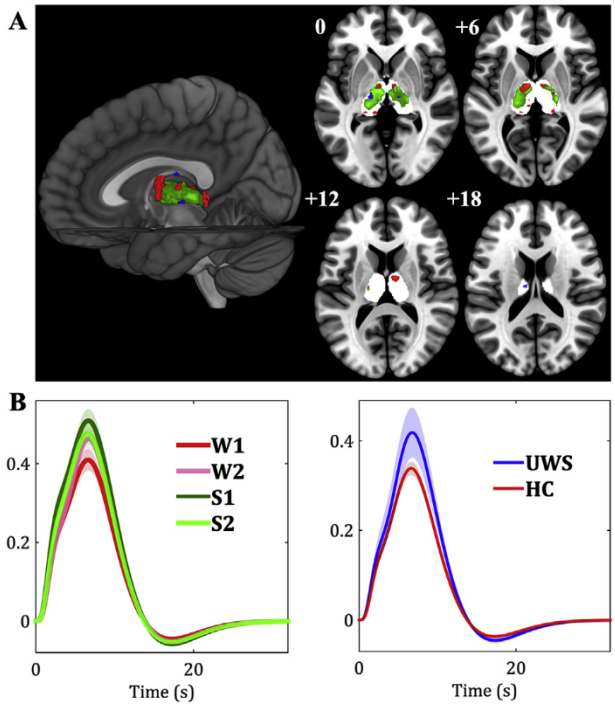

Fig. 8. (A): W1 minus S2 (positive: red, negative: blue) and healthy controls minus UWS patients (negative: green) in response height differences, $p < 0.05$, uncorrected. (B): Group averaged HRF with its standard error in voxel in the thalamus (white shadow mask), MNI coordinates: [-15, −18, 0].

4.1. Methodological considerations

Stimulus-evoked BOLD fMRI is one of the most conventional paradigms to investigate anesthetic influence on neuronal activation. Stimulus-based techniques rely on the response of specific brain regions to a given task. On the other hand unexpected (from the point of view of the design) or unspecific widespread BOLD signal changes across the brain are frequently observed. Additionally, finding a balance between complexity and applicability is always a challenge for task stimuli. Conversely, a paradigm-free approach such as resting state fMRI allows investigating the baseline activity of the whole brain. Looking for statistical dependencies across time series of brain regions (functional connectivity) is the typical analysis performed in these paradigms, and this is also true for consciousness studies. Due to relatively poor temporal resolution, few studies focus on exploring the spontaneous event dynamics of anesthesia. As shown in previous works, an efficient way to

reveal this spontaneous activity at cortical level from resting state BOLD signal could be through point process analysis, under the hypothesis that important features of brain dynamics at rest can be captured from relatively large fluctuations in BOLD amplitude (Tagliazucchi et al., 2012; Wu et al., 2013). A study on PCC related co-activations patterns by point process analysis has shown region-specific modulations in Propofol-induced anesthesia (Amico et al., 2014).

As discussed in (Di et al., 2008), due to uncontrolled head movements during scanning, the patients with UWS may show more motion artifacts than in collaborative healthy subjects. To avoid motion-related artifacts contribution to point process, 3Ddespike and aCompCor were combined to attenuate motion artifacts, to minimize the framewise relationship between head motion and signal change (Muschelli et al., 2014). To further minimize the motion artifact influence on HRF shape retrieved from point process, data scrubbing on point process detection is performed (Power et al., 2012), and mean FD power of each subject is included as a covariate for further statistical analysis (Van Dijk et al., 2012). This procedure indicates that our results are unlikely to be explained by motion artifacts. It is shown that multi-echo fMRI is a highly promising technique to distinguish BOLD signal from non-BOLD artifacts (Kundu et al., 2017). Such method may provide valuable insights on the spontaneous point process events retrieved from BOLD signal with different contrast-to-noise ratios. The results presented here might be affected by the variation in magnetic susceptibility due to the different echo times used in the two datasets (possibly explaining the differences found in the thalamus).

Physiological (cardiac, pulmonary) contributors of BOLD signal, and sources of its variability, should be taken into account, especially in resting state fMRI studies. These also influence the detection of spontaneous events and the retrieved HRF (Wu and Marinazzo, 2016), and might contribute to the autocorrelation of the residuals. The datasets used here did not contain explicit physiological measurements, nonetheless the use of aCompCor represents the next best solution. The GLM based HRF retrieving will benefit from heterogeneous distribution of temporal interval between these point process events, i.e. temporal 'jitter' variation in event onset times (Buckner, 1998), while its power is relative to violation the assumption of linear additively (Boynton et al., 1996). As shown in a simulation study, there is more bias in the estimates of FWHM and time to peak than response height (Lindquist et al., 2009). This evidence could partially explain less group level finding discovered in FWHM and time to peak. Meanwhile, our findings also suggest that hemodynamic response height shows the most discriminative power than other HRF parameters. Additionally, the coupling between neural activity and the vascular response is significant in determining the amplitude and spatial resolution of the BOLD signal (Logothetis and Wandell, 2004). Regions of sparse vascularization are likely to have low efficacy of this coupling and weak or absent BOLD response. This may be related to higher hemodynamic response height found in the cortical surface.

The threshold chosen for detecting the point process could also influence the results. Previous work on point processes in fMRI suggested that there is a wide range for which this detection is stable (see for example Fig. 1 in (Liu and Duyn, 2013)). We repeated our analyses for different values of the point process detection threshold ($m = \mu + 0.5\sigma$, $\mu + \sigma$, $\mu + 1.5\sigma$) obtaining similar statistical maps (Fig. S5).

As a last limitation, it should be mentioned that the age and scanning parameters differences could not be handled in the conjunction analysis on the two datasets.

5. Conclusions

To conclude, our results show that a proxy of neurovascular coupling in different states of consciousness could be tracked by modulated spontaneous hemodynamic response derived from resting state fMRI. These results demonstrate the feasibility of resting state HRF for the study of the brain at rest, revealing comprehensive and complementary information to further decode anesthetic and pathological brain function, especially for clinical populations and conditions not suitable for PET imaging.

Acknowledgements

G-R.W was supported by the National Natural Science Foundation of China (Grant No. 61876156). D.M. was supported by the Fonds Wetenschappelijk Onderzoek Flanders, Belgium, grant n. G036716N.

The Coma Science Group acknowledges the Belgian National Funds for Scientific Research (FRS-FNRS), European Commission, Luminous (EU-H2020-fetopenga686764), Center-TBI, the European Union's Horizon 2020 Framework Programme for Research and Innovation under the Specific Grant Agreement No. 785907 (Human Brain Project SGA2), James McDonnell Foundation-United States, European Space Agency, Belspo, "Fondazione Europea Ricerca Biomedica," (Italy-Europe) BIAL Foundation, Portugal, Wallonia-Brussels Federation Concerted Research Action, and Mind Science Foundation.

Appendix A. Supplementary data

Supplementary data to this article can be found online at https://doi.org/10.1016/j.neuroimage.2019.07.011.

References

Alkire, M.T., Hudetz, A.G., Tononi, G., 2008. Consciousness and anesthesia. Science 322, 876–880.
Alkire, M.T., Miller, J., 2005. General anesthesia and the neural correlates of consciousness. Prog. Brain Res. 150, 229–244.
Amico, E., Gomez, F., Di Perri, C., Vanhaudenhuyse, A., Lesenfants, D., Boveroux, P., Bonhomme, V., Brichant, J.F., Marinazzo, D., Laureys, S., 2014. Posterior cingulate cortex-related co-activation patterns: a resting state FMRI study in propofol-induced loss of consciousness. PLoS One 9, e100012.
Behzadi, Y., Restom, K., Liau, J., Liu, T.T., 2007. A component based noise correction method (CompCor) for BOLD and perfusion based fMRI. Neuroimage 37, 90–101.
Boly, M., Garrido, M.I., Gosseries, O., Bruno, M.A., Boveroux, P., Schnakers, C., Massimini, M., Litvak, V., Laureys, S., Friston, K., 2011. Preserved feedforward but impaired top-down processes in the vegetative state. Science 332, 858–862.
Boveroux, P., Vanhaudenhuyse, A., Bruno, M.A., Noirhomme, Q., Lauwick, S., Luxen, A., Degueldre, C., Plenevaux, A., Schnakers, C., Phillips, C., Brichant, J.F., Bonhomme, V., Maquet, P., Greicius, M.D., Laureys, S., Boly, M., 2010. Breakdown of within- and between-network resting state functional magnetic resonance imaging connectivity during propofol-induced loss of consciousness. Anesthesiology 113, 1038–1053.
Boynton, G.M., Engel, S.A., Glover, G.H., Heeger, D.J., 1996. Linear systems analysis of functional magnetic resonance imaging in human V1. J. Neurosci. 16, 4207–4221.
Brown, E.N., Lydic, R., Schiff, N.D., 2010. General anesthesia, sleep, and coma. N. Engl. J. Med. 363, 2638–2650.
Buckner, R.L., 1998. Event-related fMRI and the hemodynamic response. Hum. Brain Mapp. 6, 373–377.
Chen, G., Saad, Z.S., Adleman, N.E., Leibenluft, E., Cox, R.W., 2015. Detecting the subtle shape differences in hemodynamic responses at the group level. Front. Neurosci. 9.
Chumbley, J., Worsley, K., Flandin, G., Friston, K., 2010. Topological FDR for neuroimaging. Neuroimage 49, 3057–3064.
Dale, A.M., Buckner, R.L., 1997. Selective averaging of rapidly presented individual trials using fMRI. Hum. Brain Mapp. 5, 329–340.
Di, H., Boly, M., Weng, X., Ledoux, D., Laureys, S., 2008. Neuroimaging activation studies in the vegetative state: predictors of recovery? Clin. Med. 8, 502–507.
Di Perri, C., Bastianello, S., Bartsch, A.J., Pistarini, C., Maggioni, G., Magrassi, L., Imberti, R., Pichiecchio, A., Vitali, P., Laureys, S., Di Salle, F., 2013. Limbic hyperconnectivity in the vegetative state. Neurology 81, 1417–1424.
DiFrancesco, M.W., Robertson, S.A., Karunanayaka, P., Holland, S.K., 2013. BOLD fMRI in infants under sedation: comparing the impact of pentobarbital and propofol on auditory and language activation. J. Magn. Reson. Imaging 38, 1184–1195.
Fiset, P., Plourde, G., Backman, S.B., 2005. Brain imaging in research on anesthetic mechanisms: studies with propofol. Prog. Brain Res. 150, 245–250.
Friston, K.J., Fletcher, P., Josephs, O., Holmes, A., Rugg, M.D., Turner, R., 1998. Event-related fMRI: characterizing differential responses. Neuroimage 7, 30–40.
Giacino, J.T., Kalmar, K., Whyte, J., 2004. The JFK Coma Recovery Scale-Revised: measurement characteristics and diagnostic utility. Arch. Phys. Med. Rehabil. 85, 2020–2029.
Gitelman, D.R., Penny, W.D., Ashburner, J., Friston, K.J., 2003. Modeling regional and psychophysiologic interactions in fMRI: the importance of hemodynamic deconvolution. Neuroimage 19, 200–207.
Gugino, L.D., Chabot, R.J., Prichep, L.S., John, E.R., Formanek, V., Aglio, L.S., 2001. Quantitative EEG changes associated with loss and return of consciousness in healthy adult volunteers anaesthetized with propofol or sevoflurane. Br. J. Anaesth. 87, 421–428.

Guldenmund, P., Demertzi, A., Boveroux, P., Boly, M., Vanhaudenhuyse, A., Bruno, M.A., Gosseries, O., Noirhomme, Q., Brichant, J.F., Bonhomme, V., Laureys, S., Soddu, A., 2013. Thalamus, brainstem and salience network connectivity changes during propofol-induced sedation and unconsciousness. Brain Connect. 3, 273–285.
Gusnard, D.A., Raichle, M.E., Raichle, M.E., 2001. Searching for a baseline: functional imaging and the resting human brain. Nat. Rev. Neurosci. 2, 685–694.
Hudetz, A.G., 2012. General anesthesia and human brain connectivity. Brain Connect. 2, 291–302.
Kundu, P., Voon, V., Balchandani, P., Lombardo, M.V., Poser, B.A., Bandettini, P.A., 2017. Multi-echo fMRI: a review of applications in fMRI denoising and analysis of BOLD signals. Neuroimage 154, 59–80.
Laureys, S., 2005. The neural correlate of (un)awareness: lessons from the vegetative state. Trends Cognit. Sci. 9, 556–559.
Laureys, S., Faymonville, M.E., Degueldre, C., Fiore, G.D., Damas, P., Lambermont, B., Janssens, N., Aerts, J., Franck, G., Luxen, A., Moonen, G., Lamy, M., Maquet, P., 2000a. Auditory processing in the vegetative state. Brain 123 (Pt 8), 1589–1601.
Laureys, S., Faymonville, M.E., Luxen, A., Lamy, M., Franck, G., Maquet, P., 2000b. Restoration of thalamocortical connectivity after recovery from persistent vegetative state. Lancet 355, 1790–1791.
Laureys, S., Faymonville, M.E., Peigneux, P., Damas, P., Lambermont, B., Del Fiore, G., Degueldre, C., Aerts, J., Luxen, A., Franck, G., Lamy, M., Moonen, G., Maquet, P., 2002. Cortical processing of noxious somatosensory stimuli in the persistent vegetative state. Neuroimage 17, 732–741.
Laureys, S., Goldman, S., Phillips, C., Van Bogaert, P., Aerts, J., Luxen, A., Franck, G., Maquet, P., 1999a. Impaired effective cortical connectivity in vegetative state: preliminary investigation using PET. Neuroimage 9, 377–382.
Laureys, S., Lemaire, C., Maquet, P., Phillips, C., Franck, G., 1999b. Cerebral metabolism during vegetative state and after recovery to consciousness. J. Neurol. Neurosurg. Psychiatry 67, 121.
Laureys, S., Owen, A.M., Schiff, N.D., 2004. Brain function in coma, vegetative state, and related disorders. Lancet Neurol. 3, 537–546.
Laureys, S., Schiff, N.D., 2012. Coma and consciousness: paradigms (re)framed by neuroimaging. Neuroimage 61, 478–491.
Leech, R., Braga, R., Sharp, D.J., 2012. Echoes of the brain within the posterior cingulate cortex. J. Neurosci. 32, 215–222.
Lindquist, M.A., Meng Loh, J., Atlas, L.Y., Wager, T.D., 2009. Modeling the hemodynamic response function in fMRI: efficiency, bias and mis-modeling. Neuroimage 45, S187–S198.
Lindquist, M.A., Wager, T.D., 2007. Validity and power in hemodynamic response modeling: a comparison study and a new approach. Hum. Brain Mapp. 28, 764–784.
Liu, X., Duyn, J.H., 2013. Time-varying functional network information extracted from brief instances of spontaneous brain activity. Proc. Natl. Acad. Sci. U. S. A. 110, 4392–4397.
Logothetis, N.K., Wandell, B.A., 2004. Interpreting the BOLD signal. Annu. Rev. Physiol. 66, 735–769.
Menon, D.K., Owen, A.M., Pickard, J.D., 1999. Response from menon, owen and pickard. Trends Cognit. Sci. 3, 44–46.
Muschelli, J., Nebel, M.B., Caffo, B.S., Barber, A.D., Pekar, J.J., Mostofsky, S.H., 2014. Reduction of motion-related artifacts in resting state fMRI using aCompCor. Neuroimage 96, 22–35.
Nakayama, N., Okumura, A., Shinoda, J., Nakashima, T., Iwama, T., 2006. Relationship between regional cerebral metabolism and consciousness disturbance in traumatic diffuse brain injury without large focal lesions: an FDG-PET study with statistical parametric mapping analysis. J. Neurol. Neurosurg. Psychiatry 77, 856–862.
Nichols, T., Brett, M., Andersson, J., Wager, T., Poline, J.B., 2005. Valid conjunction inference with the minimum statistic. Neuroimage 25, 653–660.
Ogawa, S., Lee, T.M., Kay, A.R., Tank, D.W., 1990. Brain magnetic resonance imaging with contrast dependent on blood oxygenation. Proc. Natl. Acad. Sci. U. S. A. 87, 9868–9872.
Owen, A.M., Coleman, M.R., Menon, D.K., Berry, E.L., Johnsrude, I.S., Rodd, J.M., Davis, M.H., Pickard, J.D., 2005. Using a hierarchical approach to investigate residual auditory cognition in persistent vegetative state. Prog. Brain Res. 150, 457–471.
Power, J.D., Barnes, K.A., Snyder, A.Z., Schlaggar, B.L., Petersen, S.E., 2012. Spurious but systematic correlations in functional connectivity MRI networks arise from subject motion. Neuroimage 59, 2142–2154.
Quan, X., Yi, J., Ye, T.H., Tian, S.Y., Zou, L., Yu, X.R., Huang, Y.G., 2013. Propofol and memory: a study using a process dissociation procedure and functional magnetic resonance imaging. Anaesthesia 68, 391–399.
Raichle, M.E., 2015. The brain's default mode network. Annu. Rev. Neurosci. 38, 433–447.
Rangaprakash, D., Dretsch, M.N., Yan, W., Katz, J.S., Denney Jr., T.S., Deshpande, G., 2017. Hemodynamic variability in soldiers with trauma: implications for functional MRI connectivity studies. Neuroimage Clin 16, 409–417.
Rangaprakash, D., Wu, G.R., Marinazzo, D., Hu, X., Deshpande, G., 2018. Hemodynamic response function (HRF) variability confounds resting-state fMRI functional connectivity. In: Magnetic Resonance in Medicine.
Schiff, N.D., 2008. Central thalamic contributions to arousal regulation and neurological disorders of consciousness. Ann. N. Y. Acad. Sci. 1129, 105–118.
Schiff, N.D., Plum, F., 1999. Cortical function in the persistent vegetative state. Trends Cognit. Sci. 3, 43–44.
Stender, J., Gosseries, O., Bruno, M.A., Charland-Verville, V., Vanhaudenhuyse, A., Demertzi, A., Chatelle, C., Thonnard, M., Thibaut, A., Heine, L., Soddu, A., Boly, M., Schnakers, C., Gjedde, A., Laureys, S., 2014. Diagnostic precision of PET imaging and functional MRI in disorders of consciousness: a clinical validation study. Lancet 384, 514–522.
Sun, X., Zhang, H., Gao, C., Zhang, G., Xu, L., Lv, M., Chai, W., 2008. Imaging the effects of propofol on human cerebral glucose metabolism using positron emission tomography. J. Int. Med. Res. 36, 1305–1310.
Tagliazucchi, E., Balenzuela, P., Fraiman, D., Chialvo, D.R., 2012. Criticality in large-scale brain FMRI dynamics unveiled by a novel point process analysis. Front. Physiol. 3, 15.
Tak, S., Wang, D.J., Polimeni, J.R., Yan, L., Chen, J.J., 2014. Dynamic and static contributions of the cerebrovasculature to the resting-state BOLD signal. Neuroimage 84, 672–680.
Tomasi, D., Volkow, N.D., 2018. Association between brain activation and functional connectivity. Cerebr. Cortex 29 (5), 1984–1996. https://doi.org/10.1093/cercor/bhy077.
Tzourio-Mazoyer, N., Landeau, B., Papathanassiou, D., Crivello, F., Etard, O., Delcroix, N., Mazoyer, B., Joliot, M., 2002. Automated anatomical labeling of activations in SPM using a macroscopic anatomical parcellation of the MNI MRI single-subject brain. Neuroimage 15, 273–289.
Van Dijk, K.R., Sabuncu, M.R., Buckner, R.L., 2012. The influence of head motion on intrinsic functional connectivity MRI. Neuroimage 59, 431–438.
Vijayan, S., Ching, S., Purdon, P.L., Brown, E.N., Kopell, N.J., 2013. Thalamocortical mechanisms for the anteriorization of alpha rhythms during propofol-induced unconsciousness. J. Neurosci. 33, 11070–11075.
Wannez, S., Gosseries, O., Azzolini, D., Martial, C., Cassol, H., Aubinet, C., Annen, J., Martens, G., Bodart, O., Heine, L., Charland-Verville, V., Thibaut, A., Chatelle, C., Vanhaudenhuyse, A., Demertzi, A., Schnakers, C., Donneau, A.F., Laureys, S., 2017. Prevalence of coma-recovery scale-revised signs of consciousness in patients in minimally conscious state. Neuropsychol. Rehabil. 1–10.
Ward, L.M., 2011. The thalamic dynamic core theory of conscious experience. Conscious. Cognit. 20, 464–486.
Wu, G.R., Liao, W., Stramaglia, S., Ding, J.R., Chen, H., Marinazzo, D., 2013. A blind deconvolution approach to recover effective connectivity brain networks from resting state fMRI data. Med. Image Anal. 17, 365–374.
Wu, G.R., Marinazzo, D., 2015. Retrieving the hemodynamic response function in resting state fMRI: methodology and application. PeerJ PrePrints 3, e1621.
Wu, G.R., Marinazzo, D., 2016. Sensitivity of the resting-state haemodynamic response function estimation to autonomic nervous system fluctuations. Philos Trans A Math Phys Eng Sci 374, 028514.
Yan, W., Rangaprakash, D., Deshpande, G., 2018. Aberrant hemodynamic responses in autism: implications for resting state fMRI functional connectivity studies. Neuroimage: Clinical 19, 320–330.